Physicochem. Probl. Miner. Process., 61(5), 2025, 210645

http://www.journalssystem.com/ppmp

Physicochemical Problems of Mineral Processing

ISSN 1643-1049

Flow field analysis and engineering application of the turbulence-forced pulp conditioner

Hainan Wang [1,2,3], Ruifeng Chen [1,2,3], Danlong Li [1], Qinggang Zeng [4], Xiancai Wen [4], Jiawei Lv [4], Xiaokang Yan [1,2,3], Jincai Ran [2,3,5], Haijun Zhang [1,2,3]

[1] School of Chemical Engineering and Technology, China University of Mining and Technology, Xuzhou 221116, Jiangsu, China

[2] National Engineering Research Center of Coal Preparation & Purification, China University of Mining & Technology, Xuzhou 221116 Jiangsu, China

[3] State Key Laboratory of Coking Coal Resources Green Exploitation, China University of Mining and Technology, Xuzhou 221116, China

[4] Bakuang Coal Preparation Plant, PingDingShan TianAn Coal Co.Ltd, Pingdingshan 467000, China

[5] School of Mining Engineering and Geology, Xinjiang Institute of Engineering, Urumqi 830023, Xinjiang, China

Corresponding authors: Wanghainan07@163.com (H. Wang), zhjcumt@163.com (H. Zhang)

Abstract: During flotation, a sufficient difference in the surface hydrophobicity of various particles is the key to completing selective separation. The quest for collector adsorption on objective particle surfaces has attracted substantial attention, but faces serious challenges regarding fine slimes with low mass and inertia. To improve the reagent interaction with coal particles, this study developed a Turbulence-Forced Pulp Conditioner (*TFPC*) that intensifies turbulent shear through multi-stage impellers. Flow field characteristics of the *TFPC* were analyzed using Computational Fluid Dynamics (*CFD*) numerical simulations. The conditioning performance was examined by the contact angle measurements and practical flotation experiments. Results showed that agitation frequency at 39 Hz created zones with high turbulent kinetic energy and dissipation, which is necessary for micro-mixing by lowering the Kolmogorov eddy scale across the device below 50 μm. Compared with the previous conditioning device, the *TFPC* significantly decreased the consumption of flotation reagents by more than 40%, and meanwhile obtained a better surface hydrophobization effect, thus contributing to increasing the cleaned coal yield. Owing to the improved cleaned coal recovery and reagent savings, *TFPC* can produce a net economic benefit despite the increase in energy consumption. This work is expected to promote the understanding of hydrodynamic enhancement during fine coal flotation and provide significant references for the process optimization in industrial applications.

Keywords: flotation, pulp conditioning, fine coal, industrial application

1. Introduction

As a fundamental energy source in China, coal plays an indispensable role in national economic development (Bhattacharya et al., 2015; Chen et al., 2022; Chen et al., 2025). However, coal resources of China are relatively poor in quality (Chen et al., 2018; Song et al., 2019; Wang et al., 2021), and meanwhile, continuous high-intensity mining has led to the gradual depletion of high-quality reserves, making low-grade coal with high ash content and impurities become the primary target for future resource recovery (Wang et al., 2025a). If the coal is not properly separated prior to utilization, it will cause a pollution hazard that influences the quality of soil, air, and water. To address this challenge, there is an urgent need to develop efficient coal upgrading and deep separation technologies. While advances in dense-medium coal separation have greatly increased the efficiency of coarse coal processing, the effective separation of fine-grained coal remains a bottleneck limiting the efficient usage of low-grade resources (Meshram et al., 2015; Behera et al., 2018; Yu et al., 2023). One of the major methods for the separation of fine coal is flotation, which uses differences in particle surface

DOI: 10.37190/ppmp/210645

hydrophobicity within a complex gas-liquid-solid three-phase system to recover cleaned coal (Zhu et al., 2020; Wang et al., 2020; Li et al., 2024; Wang et al., 2025b). Therefore, increasing the surface hydrophobicity of ultrafine coal slime is critical for improving flotation efficiency (Xia et al., 2014; Li et al., 2020; Zhuo et al., 2023).

Pulp conditioning, an essential process prior to flotation, aims at ensuring dispersion and homogeneity of particles and reagents (López et al., 2022). It helps improve effective reagent adsorption on target mineral surfaces and enhances surface property differences between valuable components and unwanted gangue, thereby producing suitable interfacial conditions for subsequent separation process (Quast, 2015; Wang et al., 2022; Xue et al., 2022). Previous literature has shown that high-intensity conditioning produces high fluid shear rates, efficiently dispersing particles and reagents, improving mineral floatability, and increasing recovery (Engel et al., 1997; Huang et al., 2012; Li et al., 2025a). It is further revealed that significant shear pressures effectively remove kaolinite and other clay mineral covering layers from coal surfaces, thereby increasing the direct adsorption area for collectors (Yu et al., 2017). Nevertheless, nonpolar collector adsorption on coal surfaces is essentially physical, with weak bonding forces to prevent desorption (Zhou et al., 2024). Ni et al. (2018) investigated how particle collision probability, bypass probability, and desorption probability influence effective collector adsorption probability, showing that conditioning energy input must be optimized; either too much or too little energy impairs flotation efficiency.

As the understanding of hydrodynamics in pulp conditioning advances, some novel high-efficiency conditioning devices have been developed. For example, a dual-impeller pitched-blade open-turbine forced mixer was designed to improve mixing efficiency by increasing energy input (Gui et al., 2013). A multi-nozzle ducted jet conditioning system was developed to improve reagent emulsification, dispersion, and particle collision (Wang et al., 2025c). A flow mixer with multi-stage counter-rotating cyclone tubes was devised to promote particle dispersion and increase mixing uniformity (Li et al., 2022). Additionally, different flow patterns have also been employed to create locally strong turbulent zones, magnifying velocity gradients and strengthening adsorption, including the high-speed impact flow (Wang et al., 2020) and head-on collision flow (Chen et al., 2023). Experimental validation and *CFD* simulations showed that the high velocity gradient in the inner cylinder collision zone of the CFPCD device creates a high strain rate and turbulence, which greatly improves pulp homogenization and particle-collector interactions and, ultimately, flotation performance. Additionally, for materials such as fine coal with complicated mineral distribution and ultra-fine particle sizes, they tend to exhibit low mass, low inertia, and a high bypass propensity, which impedes effective reagent interaction (Wei et al., 2023; Zhang et al., 2024; Ma et al., 2025). Specialized pretreatment techniques have been shown to be successful in improving reagent dispersion and eliminating contaminants from unburned carbon surfaces, but their widespread industrial use is fraught with difficulties (Liu et al., 2017). Therefore, it is crucial to construct the hydrodynamic environment of the conditioning process and create an appropriate flow field for reagent adsorption (Amin et al., 2014).

In light of this scenario, a Turbulence-Forced Pulp Conditioner (*TFPC*) is designed in this study. This apparatus intensifies the contacts between coal particles and collection droplets by using powerful shear forces produced by multi-stage forced impellers. The flow field properties of the *TFPC*, including velocity, pressure, turbulent kinetic energy, dissipation rate, and vorticity, were examined using numerical simulations of computational fluid dynamics (*CFD*). To confirm that impinging-flow conditioning improves coal flotation performance, industrial trials were carried out. The present study aimed to provide theoretical support and practical direction for the efficient flotation separation of fine coal, as well as the industrial development of conditioning technology.

2. Construction of the turbulence-forced pulp conditioning process

2.1. Pulp conditioning device

Fig. 1 depicts the schematic diagram of the *TFPC*. This equipment uses a synergistic integration of pipe flow, colliding flow, and agitation flow to create a multi-scale turbulent conditioning process with rationally distributed macro- and micro-eddies. Flow disruptors provide strong velocity gradients and shear friction, giving rise to energy-containing micro-eddies that can enhance the removal of impurities on particle surfaces, and oily reagent dispersion, as well as the efficient reagent adsorption/spreading

on coal surfaces. Upon operation, the pulp initially enters the main body of the device through the feed pipe, which is evenly distributed to six impinging pipes via a distribution ring. Subsequently, the pulp is rapidly released from the colliding pipes, creating a powerful impact flow field in the lower part of the cylinder. Subsequently, the pulp is dispersed in the space between the two lowest annular plates after being drawn into the suction impeller. In this stage, the pulp is mixed with pre-adjusted flotation reagents that have been drawn into the reagent pipe. The forced impeller then pushes the pulp and reagent mixture upward into the top impeller action zone. The radial impeller agitates the pulp in this instance, and the uppermost forced impeller then intensifies the conditioning process. The conditioned pulp can be released through the outlet pipe.

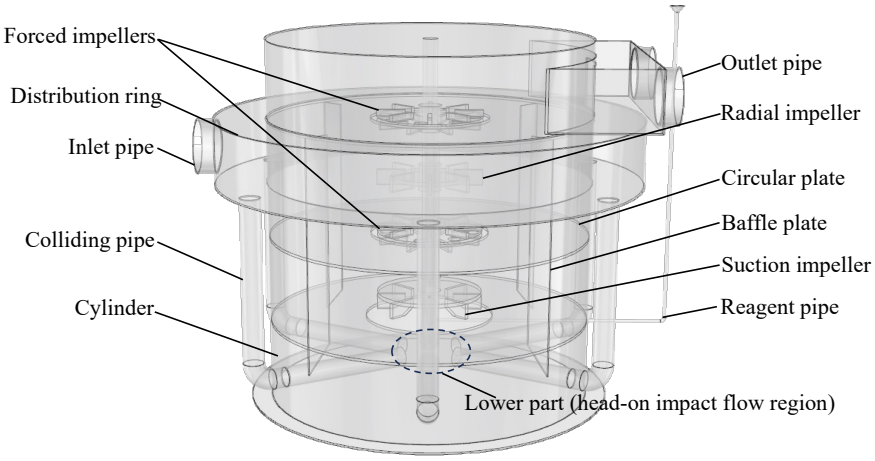

Fig. 1. Schematic diagram of the *TFPC*

2.2. Numerical simulation

UG NX software was used to obtain a three-dimensional geometric model of the *TFPC* structure shown in Fig. 1. ANSYS ICEM *CFD* software was then employed to discretize this model into an unstructured mesh that was dominated by tetrahedral components. A thorough grid independence analysis was carried out to guarantee the accuracy of the numerical simulation and eliminate the effect of grid density. For this validation, the volume-averaged turbulent dissipation rate (ε_v) was used as the primary factor. The change in ε_v as the number of total mesh increases is depicted in Fig. 2. As the mesh was further improved, the calculated ε_v values showed an increasing trend. When the overall mesh count reached 2,203,991, the ε_v values became basically stabilized. This stability shows that under this condition, the solution is insensitive to additional mesh refinement, indicating that the spatial resolution is adequate to represent the key features of turbulent dissipation in the flow field. As such, the mesh configuration with the number of 2,203,991 was chosen for further numerical simulations based on the dual criteria of computational precision and resource limitations.

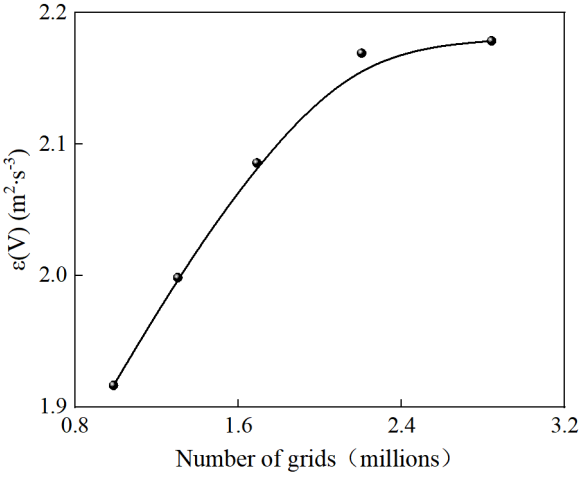

Fig. 2. Grid independence verification

Gravitational influences were taken into consideration when simulating flow fields using the ANSYS Fluent software. The boundary conditions included a pressure outlet (relative static pressure: 0 Pa) and a velocity inlet (gauge pressure: 0 Pa and turbulence intensity: 5%). The turbulent viscosity ratio (the ratio between the turbulent viscosity and the molecular dynamic viscosity) was set at 10. The liquid-phase flow was resolved by the Euler-Euler multiphase model, whilst the usual k-epsilon model was used to close the turbulence. The SIMPLE technique was used for the pressure-velocity coupling, and the Least Squares Cell-Based method was used to calculate the gradients. The Second Order Upwind technique for pressure, momentum, turbulent kinetic energy (k), and turbulent dissipation rate (ε) was selected for spatial discretization. Iterations were carried out until the residuals of all governing equations fell below 10^{-4}, indicating that steady-state convergence had been reached. Upon convergence, detailed quantitative and qualitative analyses of key flow characteristics, including velocity, pressure, turbulent kinetic energy, and turbulent dissipation rate fields within the *TFPC*, could be obtained.

2.3. Materials

The test sample was collected from a coal preparation plant of the Pingmei Shenma Group. The raw coal was dried, prepared, and divided for further testing and analysis. Table 1 presents the proximate and final analysis results for the dried coal sample. Proximate analysis (air-dried basis) indicated that the moisture (M), ash (A), volatile matter (V), and estimated fixed carbon (FC) were 0.79%, 35.24%, 15.97%, and 48.00%, respectively. The high fixed carbon value suggests a substantial residual carbon content. Ultimate analysis (dry ash-free basis) showed a carbon content of 86.36% and an oxygen content of 6.90%. In this work, the main constituents of the collector and frother corresponded to oily types and alcohols, respectively.

Table 1. Proximate analysis and ultimate analysis

Proximate Analysis (ad, %)				**Ultimate Analysis (daf, %)**				
M	***A***	***V***	***FC #***	***C***	***H***	***N***	***S***	***O #***
0.79	35.24	15.97	48.00	86.36	4.83	1.38	0.53	6.90

daf: dry ash-free basis; #: by difference subtraction calculation

Table 2. Size analysis results of the employed coal sample

Particle Size (mm)	**Yield (%)**	**Ash Content (%)**	**Cumulative Oversize**		**Cumulative Oversize**	
			Yield (%)	**Ash (%)**	**Yield (%)**	**Ash (%)**
+0.5	0.96	10.42	0.96	10.42	100.00	32.50
-0.5+0.25	8.45	15.46	9.41	14.95	99.04	32.71
-0.25+0.125	13.95	23.19	23.36	19.87	90.59	34.32
-0.125+0.074	10.36	20.32	33.72	20.01	76.64	36.35
-0.074+0.045	9.53	30.76	43.25	22.38	66.28	38.85
-0.045	56.75	40.21	100.00	32.50	56.75	40.21
Total	100.00	32.50				

The particle size composition of the coal is presented in Table 2. It can be found that ultra-fine particles dominated the coal, accounting for 56.75% of the total sample. Notably, the ash content of this ultra-fine fraction (40.21%) exceeded the whole sample average (32.50%), contributing to more than 70% of the total ash. Analysis of the ash-by-size association revealed a clear distinction: the coarser fraction (43.25%) had a significantly lower ash content, indicating that the ultra-fine fraction should be the main bottleneck for ash control. To further examine the size distribution of particles less than 45 μm, a laser particle size analyzer (BT-9300S, China) was employed. According to the result in Fig. 3, the size fraction of -10 μm accounted for about 30% -45 μm coal sample. In this scenario, employing a proper processing strategy, with a particular emphasis on intensifying the treatment of the fine fraction, was required to maximize overall separation efficiency and cost benefit.

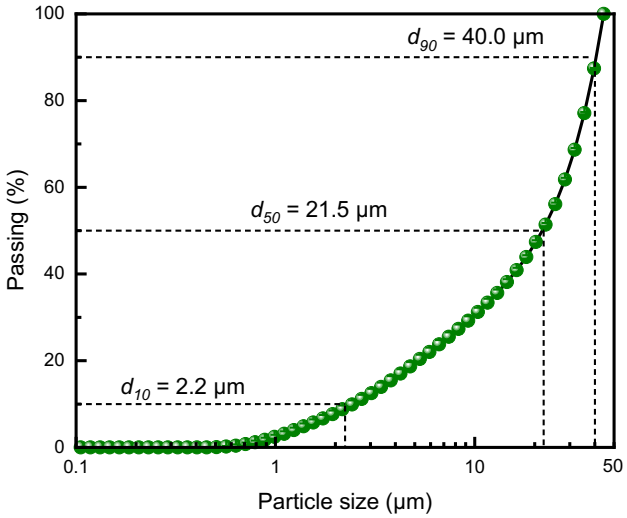

Fig. 3. Particle size distribution of -45 μm coal sample

2.4. Engineering application process

The industrial application of the *TFPC* was conducted at the Bakuang Coal Preparation Plant of the Pingdingshan Shenma Group. The feed slurry entered the *TFPC* through the gravity-driven and pressureless flow, utilizing the existing elevation difference, with a stable flow rate maintained at approximately 700 m^3/h. Upon entering the *TFPC*, the agitation system was activated. Systematic investigation of varying energy input was performed by adjusting the agitation frequency (30 Hz, 33 Hz, 36 Hz, and 39 Hz). Flotation reagents (collector and frother), metered precisely, were introduced through the reagent pipe by the significant negative pressure generated within the *TFPC*. This process effectively leveraged the internal impact collisions and high-shear forces to intensify reagent dispersion and enhance interactions with coal particle surfaces. The conditioned pulp was smoothly discharged from the topside overflow outlet, which could directly flow into the downstream flotation cells under the action of gravity for the subsequent flotation separation process. To compare the hydrophobization performance of conditioned coal particles using the previous conditioning device and the *TFPC*, contact angle values were measured by a contact angle analyzer (DSA100). Prior to each measurement, the coal sample must be pressed under a high pressure of 40 MPa for 2 min, thus giving rise to the coal plates.

3. Results and discussion

3.1. Flow velocity analysis

Fig. 4 shows the velocity distributions at the longitudinal and cross sections of the *TFPC* under different agitation frequencies. The pulp enters the feed pipe at high velocity and then flows into the expanded cross-section of the distribution ring, where it decelerates significantly and stabilizes. The stabilized pulp stream is then split and enters six pipes, resulting in a minor velocity increase. When the pulp from opposing colliding pipes meets at the cylinder bottom, they are expected to collide with each other. This counter-current action is crucial for removing fine slime from coal surfaces through inter-particle friction and enhancing reagent dispersion. The suction impeller has a considerable influence on fluid velocity in the impingement zone. Under the condition of 30 Hz, the simulation results show a relatively modest fluid velocity near the center of the colliding pipes, but the high-velocity zone expands significantly as the frequency increases to 39 Hz. The pulp is guided by the lowermost annular plate into the suction impeller zone, where the acceleration occurs.

The maximum velocity is noted behind and surrounding the lower impeller blades, and velocities behind the blades often surpass those in the immediate periphery. The suction impeller forces the pulp upward along an oblique trajectory, and the annular plates guide it into the forced impeller zone. Because of the drastically smaller flow area at the forced impeller, pulp velocity increases dramatically, significantly improving interactions between reagent particles. The pulp then flows into the radial impeller zone, which is distinguished by a large high-velocity distribution region. It then moves via the

upper forced impeller zone, into the uppermost region, and finally discharges through the overflow launder. Notably, the velocity near the reagent pipe approaches zero, demonstrating that no pulp enters this channel. Although differences in agitation frequency produce modest changes in pulp velocity magnitude, the overall spatial distribution pattern of the flow field remains fundamentally consistent.

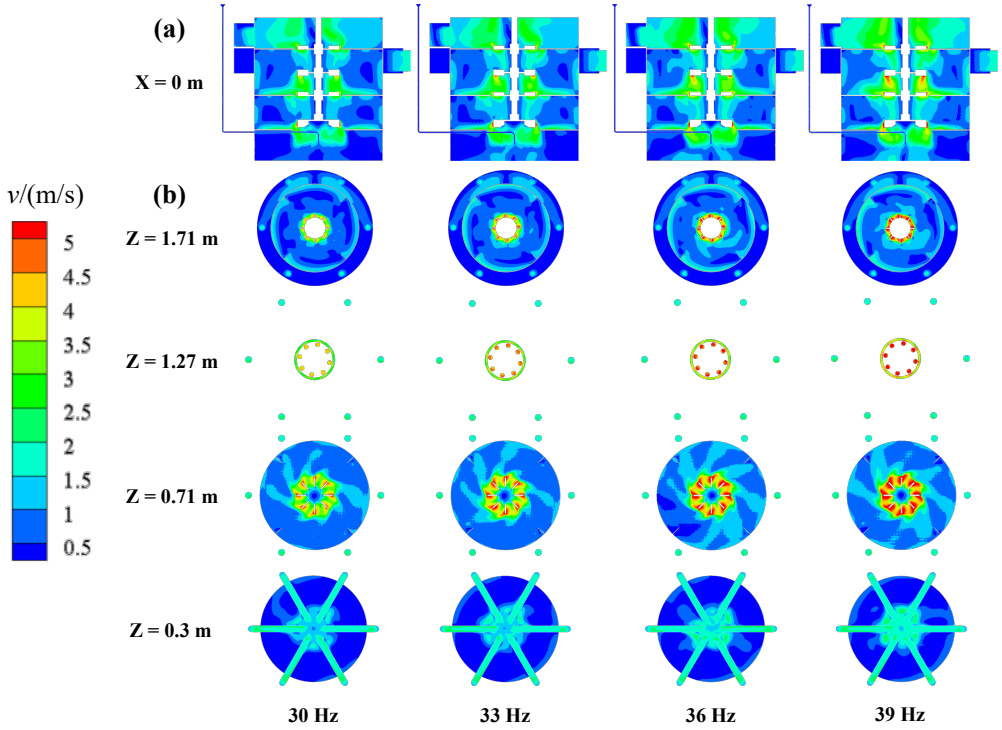

Fig. 4. Velocity distributions at the (a) longitudinal and (b) cross-section of the *TFPC* at different agitation frequencies

3.2. Pressure analysis

The pressure distributions at the longitudinal and cross sections in the *TFPC* at different agitation frequencies are shown in Fig. 5. The numerical simulations clearly show the distinctive pressure distributions for various circulation rates and agitation frequencies. The research shows that the majority of the *TFPC* cylinder is under positive pressure. Except for the impeller operating zones, pressure distributions in the entire flow area are rather consistent. Within the suction impeller zone, there is a significant reduction in pressure, resulting in a distinct low-pressure core at its center. The suction impeller creates a large negative-pressure zone in the surrounding fluid, accompanied by a significant pressure gradient, displaying excellent pulp suction capabilities.

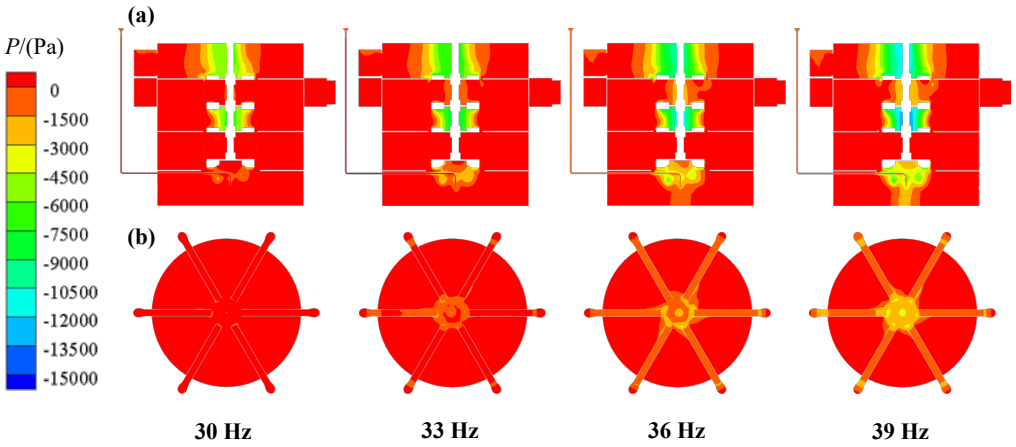

Fig. 5. Pressure distribution at the (a) longitudinal and (b) cross sections of the *TFPC* at different agitation frequencies

Notably, the agitation frequency has a significant impact on this region: below 36 Hz, the negative pressure magnitude and spatial extent are limited, whereas frequencies above 36 Hz result in a significant increase in both the magnitude of negative pressure and the affected area. Concurrently, strong negative-pressure zones and steep pressure gradients are observed between the lower forced impeller and the radial impeller, as well as the area above the upper forced impeller. This phenomenon is likely associated with the high-velocity discharge up the agitation shaft under the action of the forced impeller. Although the overall pressure distribution pattern changes little with increasing agitation frequency, absolute pressure values throughout the system grow dramatically. Crucially, the pressure at the output of the reagent pipe is constantly negative, which makes reagent suction easier. The increased negative pressure magnitude at larger agitation frequencies considerably improves the reagent suction effect (Zhang et al., 2025).

3.3. Turbulent kinetic energy and dissipation rate analysis

The distribution characteristics of turbulent kinetic energy (*TKE*) within the longitudinal section of the *TFPC* device are shown in Fig. 6, as well as the response of *TKE* to agitation frequency. Regions with relatively high *TKE* are primarily localized within the impeller zones, with peak values occurring near the blades. Agitation frequency has a significant impact on *TKE* levels: At a low frequency of 30 Hz, the *TKE* in non-impeller regions is mostly below 0.3 m^2/s^2, whereas values within impeller zones are below 1.2 m^2/s^2. Increasing the agitation frequency gradually increases the *TKE* near the impeller blades and expands the spatial extent of high-*TKE* regions within impeller zones, while the *TKE* in non-impeller regions remains relatively low. At 39 Hz, the *TKE* value of impeller zones increases significantly, typically exceeding 1.8 m^2/s^2. This clearly shows that increasing agitation intensity improves turbulence levels in the impeller regions, which is helpful for pulp mixing (Wang et al., 2025c).

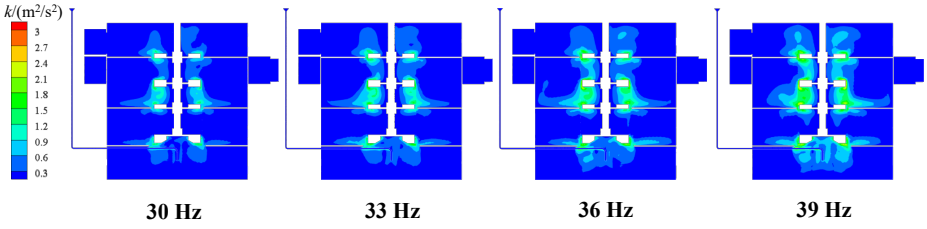

Fig. 6. Turbulent kinetic energy distribution at the longitudinal section of the *TFPC* at different agitation frequencies

Fig. 7 illustrates the distribution of the turbulent kinetic energy dissipation rate (ε) of the *TFPC* at various agitation frequencies. According to the turbulent kinetic energy distribution, regions of high dissipation rate are primarily confined to the impeller zones. This emphasizes the importance of impellers as the principal energy dissipation sources. The high-speed rotation of the suction impeller causes intense turbulent fluctuations, which efficiently transfer mechanical energy to the pulp and rapidly dissipate it within small-scale eddies. This technique provides the necessary driving power to improve microscopic interactions between particles and reagents. Furthermore, when high-velocity fluid introduced from the forced impeller impacts the radial impeller, the intervening zone experiences extreme shear, collisions, and vortex breakdown, resulting in significantly increased turbulent dissipation. The higher *TKE* traits and high ε values reinforce each other. Variations in agitation frequency have minimal impact on the spatial distribution of ε across the non-impeller region. Within the examined frequency range, the dissipation rate distribution in non-impeller regions is basically stable. The principal effect of raising frequency lies in a large increase in the energy dissipation within impeller zones. Increased agitation intensity increases ε, but does not greatly change the spatial contours of high-dissipation zones or expand their reach into non-impeller areas.

3.4. Turbulent eddy scale analysis

The Kolmogorov length scale (η), a fundamental index underlying the smallest turbulent eddies in turbulence theory, represents the characteristic size at which turbulent kinetic energy is dissipated into

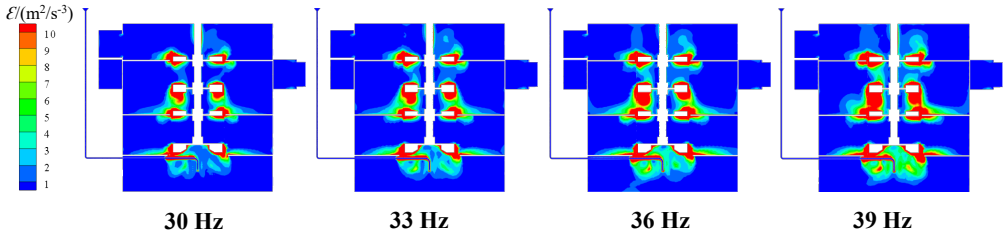

Fig. 7. Turbulent dissipation rate distribution at the longitudinal section of the *TFPC* at different agitation frequencies

internal energy through viscosity (Nguyen et al., 2016; Li et al., 2020). Its relationship with the turbulent dissipation rate is given in Eq.1:

$$\eta = \left(\frac{\upsilon^3}{\varepsilon}\right)^{1/4} \tag{1}$$

where υ is the kinematic viscosity. Fig. 8 depicts the distribution of η inside the *TFPC*. The lowest η values mainly happen in the impeller zones, indicating strong turbulent agitation on the microscale. This atmosphere considerably increases the frequency and intensity of collisions between fine coal particles and chemicals, creating ideal conditions for efficient pulp conditioning. The η values in the main flow domain of the cylinder (excluding impellers) typically ranged between 40 and 70 μm. This moderate-intensity turbulence promotes effective interaction between coal particles of relatively larger size and reagents. The overflow launcher region has larger η values, indicating a less turbulent environment. This facilitates steady pulp movement, improves macromixing, and reduces excessive particle breakage and floc disruption. Agitation frequency is an important factor for controlling microscale turbulence. Increasing frequency considerably increases the spatial extent of low-η (high-intensity) turbulent regions. At 39 Hz, η values in the inner mixing cylinder are decreased to below 50 μm, indicating increased microscale turbulence over the domain. In areas with significant shear, such as the vicinity of impellers, η values can be less than 10 μm, resulting in extraordinary micromixing. The capacity to change the spatial distribution and intensity hierarchy of η through frequency modulation is vital for increasing pulp conditioning efficacy across all particle sizes and improving reagent adsorption efficiency.

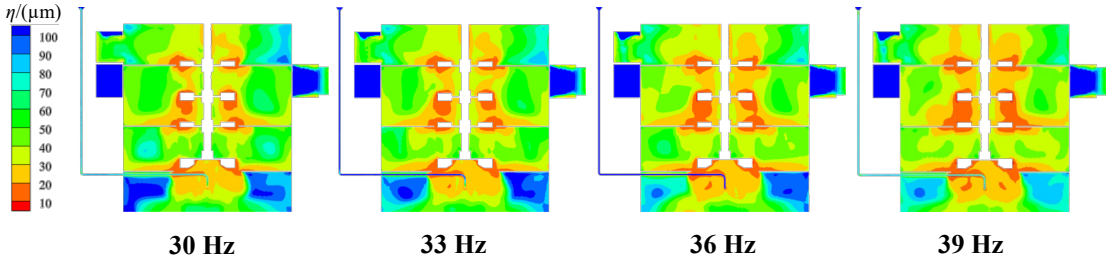

Fig. 8. Distribution of the Kolmogorov eddy scale of the *TFPC* at different agitation frequencies

3.5. Evolution analysis of turbulent eddy

Fig. 9 shows the evolution of primary and secondary vortex patterns formed in the vicinity of impellers throughout agitation frequency ranging from 30 Hz to 39 Hz. Primary tip vortices, which are prevalent around the blade tips, exhibit significant core contraction and intensification as speed increases, owing to higher centrifugal forces and tip velocity. Secondary vortical structures, particularly trailing-edge vorticity and activity at the hub, become noticeably more apparent and complex at higher speeds. Furthermore, at 39 Hz, the tip vortex exhibits instability and probable fragmentation. The uniform color scale confirms a global increase in flow velocity and intense rotational kinetic energy within the vortex cores as the agitation speeds increase. This evolution indicates significantly increased turbulent kinetic energy dissipation and flow complexity, which is directly associated with the stronger vortex dynamics and higher mixing efficiency, as well as the improved flow patterns that are crucial for process optimization.

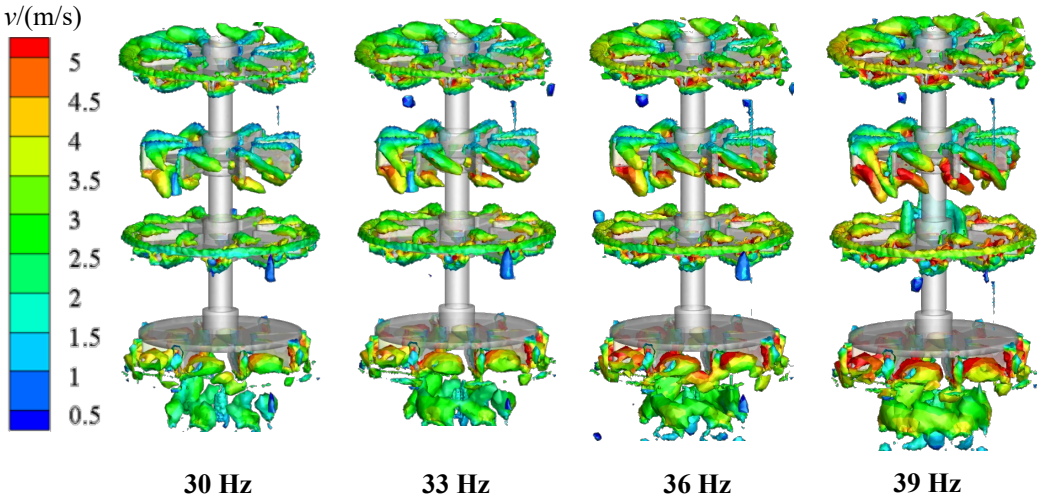

Fig. 9. Turbulent eddy evolution inside the *TFPC* at different stirring frequencies

3.6. Engineering application performance

As shown in Table 3, the industrial results clearly show that the *TFPC* outperforms the previous pulp conditioning device. At the agitation frequency ranging from 30 Hz to 36 Hz, both the recovery and ash content of concentrates obtained by two different systems exhibit a small difference in the yield and ash content of the cleaned coal, as well as the variation trend of the measured results. For example, with the agitation frequency increased from 30 Hz to 36 Hz, an obvious and consistent increase in the yield of cleaned coal could be observed. For example, the yield of cleaned coal was increased from 64.93% to 77.32% by using the *TFPC*, as opposed to the increase from 64.39% to 78.63% achieved with the previous pulp conditioning device (mixer). The improved flotation performance could be attributed to the enhanced turbulent intensity that is capable of improving particle kinetic energy and collision frequency with collector droplets. As such, the surface hydrophobicity of coal particles should be improved at a larger agitation frequency, characterized by the increased contact angle of conditioned coal from 60° to 70°.

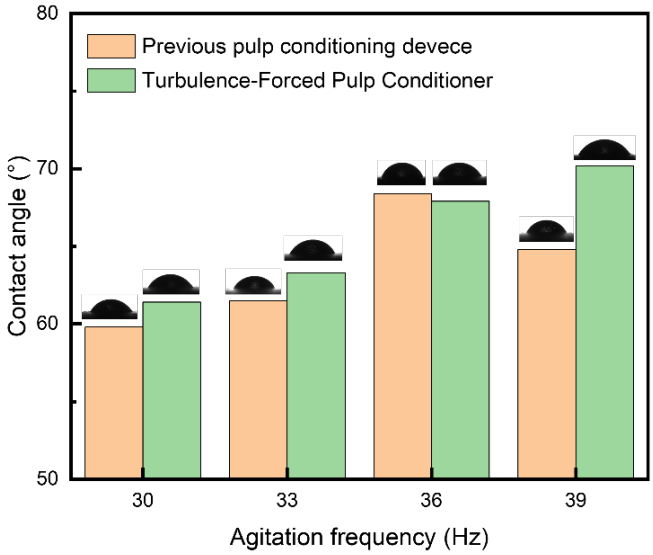

Fig. 10. Measured contact angles of conditioned coal particles under different agitation frequencies

The difference in the flotation performance of conditioned coal by the mixer and the *TFPC* occurs when the agitation frequency reaches 39 Hz, characterized by a further increased yield of concentrates from 77.32% to 78.63% using the *TFPC*, as compared to the reduced yield of concentrates from 77.63% to 73.99% employing the mixer. This result indicates that the *TFPC* requires larger energy input than

the mixer to optimize the flotation performance but obtain higher maximum yield of concentrates, evidenced by its increase from 77.63% to 78.63%. Moreover, it is indicated that different conditioning devices require proper agitation frequency to improve the particle surface hydrophobicity and thus enhance the flotation process, beyond which the yield of cleaned coal could be decreased because of excessive turbulence, causing physically adsorbed collector to detach from the coal surface. This is responsible for a decrease in the yield of concentrates from 78.63% to 73.09% when the agitation frequency increases from 39 Hz to 42 Hz.

Another advantage of the present technique is associated with its ability to considerably cut down on the flotation reagent consumption. At the agitation frequency of 30 Hz, the *TFPC* can effectively reduce the dosage of collector and frother by 12.50% and 41.44%, respectively. With increasing agitation frequency, the *TFPC* can further decrease the consumption of the collector by more than 40%. For example, regarding the insoluble oily collector, its sufficient dispersion plays a significant role in the surface hydrophobization of fine particles, evidenced by the increased contact angle in Fig. 10. By contrast, with respect to the soluble frother, it tends to adsorb at the air-water interface to maintain bubble stability. In this scenario, accompanying the overflow of the foam layer, the amount of frother remaining in pulp should decrease (Li et al., 2024). For particles with enhanced surface hydrophobicity, they should be readily captured by bubbles and become concentrated rapidly, which is expected to account for the savings in frother consumption. Consequently, by employing the *TFPC*, the reduction in reagent costs and the improvement of flotation recovery can be simultaneously achieved.

Table 3. Comparison of flotation results between *TFPC* and the original pulp conditioner

Agitation Frequency	Categories	Concentrate (%)		Tailing (%)		Collector Consumption Reduction (%)	Frother Consumption Reduction (%)
		Yield	Ash	Yield	Ash		
30 Hz	Mixer	64.39	10.18	35.61	60.20	12.50	41.44
	TFPC	64.93	10.35	35.07	60.25		
33 Hz	Mixer	65.05	10.23	34.95	60.10	17.22	48.55
	TFPC	65.66	10.34	34.34	60.13		
36 Hz	Mixer	77.63	10.71	22.37	66.63	49.10	45.76
	TFPC	77.32	10.16	22.68	63.02		
39 Hz	Mixer	73.99	10.16	26.01	65.64	44.52	41.37
	TFPC	78.63	10.36	21.37	68.56		
42 Hz	Mixer	71.89	10.38	28.11	64.84	45.16	41.15
	TFPC	73.09	10.42	26.91	67.88		

3.7. Economic analysis

The industrial application of the *TFPC* with a handling capacity of 700 m^3/h, shown in Fig. 11(a), can give rise to significant economic benefits. This technique increased the production of cleaned coal by 2.59 t/h, resulting in an annual gain of 18,648 t based on 7,200 operating hours per year. Meanwhile, the reagent consumption was significantly reduced, with the collector usage decreased by 14.62 dm^3/h and the frother usage by 11.05 dm^3/h at the agitation frequency of 39 Hz. The estimated yearly reagent cost savings could reach two million RMB (Chinese yuan), based on the regional price of 50 RMB/dm^3 for the collector and 30 RMB/dm^3 for the frother. The equipment necessitated 32 kW of electricity, leading to an additional energy consumption of 16 kWh relative to the conventional system. Through the calculation based on the industrial electricity expense of 0.8 RMB/kWh, the yearly energy cost could be increased by 92,160 RMB. Critically, the total economic result is significantly favorable, since reagent savings surpassed additional energy costs by over twenty times. Furthermore, this economic benefit could be enhanced by the revenue from the augmented production of cleaned coal, and the specific result is presented in Fig. 11(b). The synergistic enhancement of separation efficiency, indicated by a 5% increase in the yield of cleaned coal, coupled with the significant reagent reduction, facilitated complete capital investment recovery within three to six months, illustrating the exceptional cost-benefit ratio of the present technology in mineral processing applications.

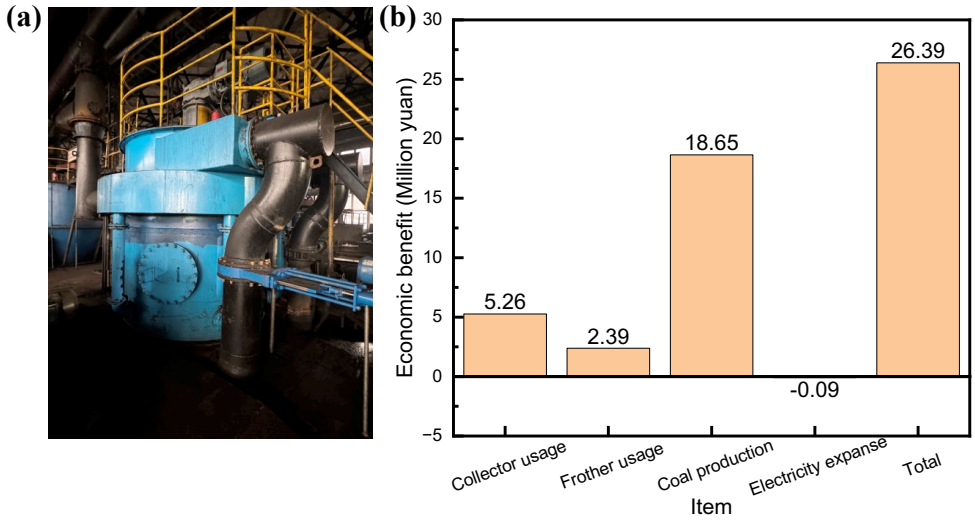

Fig. 11. (a) Turbulence-forced pulp conditioner system in the Bakuang coal preparation plant (b) Economic benefit analysis after the application of the present technique

4. Conclusions

This work studied the flow field characteristics and engineering application performance of the *TFPC* in the conditioning process of fine coal based on the combination of *CFD* numerical simulations and industrial experiments. The main conclusions are as follows:

(1) The result of numerical simulations demonstrated that the *TFPC* produces an efficient conditioning flow field by combining macro- and micro-scale vortices through multi-stage turbulence intensification. The impeller zone creates a core region with high turbulent kinetic energy and dissipation rate, giving rise to the minimum vortex scale of less than 10 μm. Given that particles tend to move with similar-sized eddies (Li et al., 2025b), the generation of small eddies is conducive to promoting the collision between fine particles and collector droplets, and improving the reagent adsorption efficiency.

(2) The *TFPC* increased the yield of cleaned coal by around 5% on average. Owing to the enhanced reagent dispersion and adsorption caused by the intense turbulence, the collector and frother consumption were significantly reduced by 44.52% and 41.37%, respectively. This effectively addresses the long-standing technical constraint of low reagent utilization efficiency by using conventional conditioning methods.

(3) With a handling capacity of 700 m^3/h, the *TFPC* can improve the production of cleaned coal by 2.59 t/h. It simultaneously saves 14.62 dm^3/h for the collector and 11.05 dm^3/h for the frother. Although operating power consumption rises by about 16 kW, the reductions in reagent costs, along with the higher value of additional clean coal output, result in a significant net economic benefit.

Acknowledgments

This work is supported by the National Key Technologies Research and Development Program (No. 2023YFC2907703), and all authors express their sincere gratitude for it.

References

AMIN, N.K., ABDEL-AZIZ, M.H., EL-ASHTOUKHY, E.Z., 2014. *Effect of pulp fiber suspensions on the rate of mass transfer controlled corrosion in pipelines under turbulent flow conditions*. Chem. Eng. Res. Des. 92, 2333-38.

BHATTACHARYA, M., RAFIQ, S., BHATTACHARYA, S., 2015. *The role of technology on the dynamics of coal consumption–economic growth: New evidence from China*. Appl. Energy. 154, 686-95.

BEHERA, S.K., MEENA, H., CHAKRABORTY, S., MEIKAP, B.C., 2018. *Application of response surface methodology (RSM) for optimization of leaching parameters for ash reduction from low-grade coal*. Int. J. Min. Sci. Technol. 28, 621-29.

CHEN, S., LI, L., QU, J., LIU, Q., TANG, L., TAO, X., FAN, H., 2018. *Oily bubble flotation technology combining modeling and optimization of parameters for enhancement of flotation of low-flame coal*. Powder Technol. 335, 171-85.

CHEN, H., LIU, K., SHI, T., WANG, L., 2022. *Coal consumption and economic growth: A Chinese city-level study*. Energy Econ. 109, 105940.

CHEN, R., WANG, H., LI, D., LIAO, Y., TIAN, Q., SU, W., LI, L., ZHANG, H., 2023. *Numerical and experimental study on the colliding flow pulp conditioning for the separation intensification of unburned carbon from coal gasification slag*. Minerals. 13(3), 398

CHEN, D., QU, B., ZHANG, J., LONG, Q., SUN, R., 2025. *Methods and techniques for determining the gas content of coal seams in China: a mini-review*. Fuel Process. Technol. 275, 108257.

ENGEL, M.D., MIDDLEBROOK, P.D., JAMESON, G.J., 1997. *Advances in the study of high intensity conditioning as a means of improving mineral flotation performance*. Miner. Eng. 10, 55-68.

GUI, X., HUANG, G., YUAN, C., LIANG, H., WANG, Y., 2013. *Mixing characteristics of two-stage compulsory stirred pulp-mixing and its influence on fine coal flotation*. Chin. J. Eng. 35, 423-31.

HUANG, G., ZHOU, C., LIU, J., 2012. *Effects of different factors during the de-silication of diaspore by direct flotation*. Int. J. Min. Sci. Technol. 22, 341-44.

LI, Y., XIA, W., PAN, L., TIAN, F., PENG, Y., XIE, G., LI, Y., 2020. *Flotation of low-rank coal using sodium oleate and sodium hexametaphosphate*. J. Clean. Prod. 261, 121216.

LI, D., WANG, H., Yang, L., Yan, X., Wang, L., Zhang, H., 2020. *Intensification effects of stirred fluid on liquid–solid, gas–liquid and gas–solid interactions in flotation: A review*. Chem. Eng. Process. 152, 107943.

LI, D., YAN, X., WANG, W., WANG, H., ZHOU, R., YANG, H., ZHANG, H., 2022. *New insights into the intensification of collector adsorption on fine particles induced by flow field*. J. Mol. Liq. 365, 120119.

LI, D., WANG, H., MANICA, R., ZHANG, Z., ZHANG, H., LIU, Q., 2024. *Quantifying contributions of different repulsion to film drainage time during the bubble–solid surface attachment and implications for the flotation of fine particles*. Langmuir. 40, 10281-92.

LI, Q., ZHOU, J., WU, Y., YANG, Y., WANG, Y., GU, G., LIU, B., 2025. *Influence of the impeller structure and operating parameters of a high intensity conditioning system on the flotation of fine-grained pyrite*. Miner Eng. 228, 109363.

LI, X., SUN, Z., WANG, H., WANG, L., YAN, X., ZHANG, H., RAN, J., LIU, J., 2025. *Particle motion under turbulent eddies: Inspiration for fine minerals flotation*. Chem. Eng. Sci. 301, 120754.

LIU, H., CHEN, Z., WANG, J., FAN, J., 2017. *The impact of resource tax reform on China's coal industry*. Energy Econ. 61, 52-61.

LOPEZ, M.P., BOTINA, B.L., GARCIA, M.C., RICO, E.M., ROMERO, Y., PEDROZA, K.J., CERON, I.X., 2022. *Reducing dead time and improving flavour profile by pulp conditioning of cacao beans*. Chem. Eng. Process. 176, 108979.

MESHRAM, P., PUROHIT, B.K., SINHA, M.K., SAHU, S.K., PANDEY, B.D., 2015. *Demineralization of low grade coal – A review*. Renew. Sust. Energy Rev. 41, 745-61.

MA, G., CUI, J., LI, J., BU, X., SHAO, H., WANG, Z., LIU, F., SOBHY, A., TAO, D., 2025. *Nanobubble enhanced flocculation and filtration of fine coal and associated mechanisms*. Fuel. 393, 134989.

NGUYEN, A.V., AN-VO, D., TRAN-CONG, T., EVANS, G.M., 2016. *A review of stochastic description of the turbulence effect on bubble-particle interactions in flotation*. Int. J. Miner. Process. 156, 75-86.

NI, C., BU, X., XIA, W., PENG, Y., XIE, G., 2018. *Effect of slimes on the flotation recovery and kinetics of coal particles*. Fuel. 220, 159-66.

QUAST, K., 2015. *Use of conditioning time to investigate the mechanisms of interactions of selected fatty acids on hematite. Part 1: Literature survey*. Miner Eng. 79, 295-300.

SONG, M., WANG, J., ZHAO, J., 2018. *Coal endowment, resource curse, and high coal-consuming industries location: Analysis based on large-scale data*. Resour. Conserv. Recy. 129, 333-44.

WANF, H., YANG, W., YAN, X., WANG, L., WANG, Y., ZHANG, H., 2020. *Regulation of bubble size in flotation: A review*. J. Environ. Chem. Eng. 8, 104070.

WANG, H., YANG, W., LI, D., ZHANG, C., YAN, X., WANG, L., ZHANG, H., 2020. *Enhancement of coal flotation using impact flow conditioning pulp*. J. Clean Prod. 267, 122124.

WANG, S., ZHAO, C., LIU, H., TIAN, X., 2021. *Exploring the spatial spillover effects of low-grade coal consumption and influencing factors in China*. Resour Policy. 70, 101906.

WANG, S., XIA, Q., XU, F., 2022. *Investigation of collector mixtures on the flotation dynamics of low-rank coal*. Fuel. 327, 125171.

WANG, Y., ZHOU, Z., LI, C., 2025. *Acclimation of phytoplankton communities to multi-scale environmental variables in subsidence wetlands created by underground coal mining in China*. Ecol. Front. 45, 127-34.

WANG, X., CUI, X., DING, R., CHENG, G., QIN, Y., ABAKA-WOOD, G., GAO, G., LI, E., CHENG, F., 2025. *Interfacial mechanism of asymmetric Gemini surfactant in synergy with kerosene for enhancing low-rank coal flotation*. Colloid. Surf. A. 722, 137267.

WANG, T., ZHOU, W., WANG, Z., LI, L., 2025. *Investigation of a jet and stirring synergistic flotation column combining two-phase flow and particle tracking simulation methods with experiments*. Powder Technol. 453, 120628.

WANG, H., CHEN, R., LI, D., ZHANG, B., YAN, X., RAN, J., ZHANG, H., 2025. *Probing the adaptability relationship between flow characteristics and mineral particles with different size and surface hydrophobicity*. Powder Technol. 452, 120588.

WEI, D., WANG, H., SI, L., TAN, C., LIU, X., YAN, H., 2023. *Point cloud registration based on the dark forest algorithm and its application in coal industry*. Appl. Soft Comput. 144, 110524.

XIA, W., XIE, G., LIANG, C., YANG, J., 2014. *Flotation behavior of different size fractions of fresh and oxidized coals*. Powder Technol. 267, 80-85.

XUE, Z., DONG, L., FAN, M., YANG, H., LIU, A., LI, Z., BAO, W., WANG, J., FAN, P., 2022. *Enhanced flotation mechanism of coal gasification fine slag with composite collectors*. Colloid. Surf. A. 641, 128593.

YU, Y., CHENG, G., MA, L., HUANG, G., WU, L., XU, H., 2017. *Effect of agitation on the interaction of coal and kaolinite in flotation*. Powder Technol. 313, 122-28.

YU, S., LI, S., GUO, P., ZHANG, Y., LI, W., WANG, H., SHI, W., JIANG, H., DUAN, C., 2023. *Research on highly efficient quality improvement process and product blending scheme for fine coal*. Powder Technol. 430, 119011.

ZHANG, T., WANG, H., TANG, J., GAO, S., 2024. *Mechanical and environmental performance of structural concrete with coal gangue fine aggregate*. J. Build. Eng. 84, 108488.

ZHANG, M., SHEN, Z., MA, F., ZHANG, Y., LIU, B., 2025. *Study of the scale-up method and dynamic performance of the forced-air self-aspirating flotation machine*. Processes, 13, 1316.

ZHUO, X., SU, J., XU, H., WANG, L., WANG, W., ZHANG, B., NI, Z., 2023. *Synergistically effective flotation enrichment of vitrinite by Na removal for high-Na high-inertinite low-rank Zhundong coal*. J. Clean. Prod. 428, 139433.

ZHOU, Y., YU, W., LI, Y., LEI, Q., XIE, H., 2024. *Power generation device via solar collector coupled with a shape-memory alloy thermo-mechanical switch utilizing MXene nanofluid as high-efficiency photothermal conversion working medium*. Energy Convers. Manag. 302, 118092.

ZHU, X., WANG, D., NI, Y., WANG, J., NIE, C., YANG, C., LYU, X., QIU, J., LI, L., 2020. *Cleaner approach to fine coal flotation by renewable collectors prepared by waste oil transesterification*. J. Clean. Prod. 252, 119822.